arXiv:1107.5925v2 [hep-ph] 27 Nov 2011

Light cone QCD sum rules study of the semileptonic heavy Ξ_Q and Ξ'_Q transitions to Ξ and Σ baryons

K. Azizi[a] *, Y. Sarac[b] †, H. Sundu[c] ‡

[a] Physics Department, Doğuş University, Acıbadem-Kadıköy, 34722 Istanbul, Turkey

[b] Electrical and Electronics Engineering Department, Atilim University, 06836 Ankara, Turkey

[c] Department of Physics, Kocaeli University, 41380 Izmit, Turkey

Abstract

The semileptonic decays of heavy spin–1/2, $\Xi_{b(c)}$ and $\Xi'_{b(c)}$ baryons to the light spin– 1/2, Ξ and Σ baryons are investigated in the framework of light cone QCD sum rules. In particular, using the most general form of the interpolating currents for the heavy baryons as well as the distribution amplitudes of the Ξ and Σ baryons, we calculate all form factors entering the matrix elements of the corresponding effective Hamiltonians in full QCD. Having calculated the responsible form factors, we evaluate the decay rates and branching fractions of the related transitions.

PACS number(s): 11.55.Hx, 13.30.Ce, 14.20.Mr, 14.20.Lq

---

*e-mail: kazizi@dogus.edu.tr

†e-mail: ysoymak@atilim.edu.tr

‡e-mail: hayriye.sundu@kocaeli.edu.tr

1 Introduction

Almost all of the anti-triplet states Λ_c^+, Ξ_c^+, Ξ_c^0 [$\Lambda_c^+(2593)$, $\Xi_c^+(2790)$, $\Xi_c^0(2790)$] with $J^P = \frac{1}{2}^+$ [$\frac{1}{2}^-$] and containing single heavy charm quark as well as the $\frac{1}{2}^+$ [$\frac{3}{2}^+$] sextet $\Omega_c, \Sigma_c, \Xi_c'$ [$\Omega_c^*, \Sigma_c^*, \Xi_c^*$] states have been detected in the experiments [1]. Among the S–wave bottom baryons, the Λ_b, Σ_b, Σ_b^*, Ξ_b and Ω_b states have also been observed. It is expected that the LHC not only will open new horizons in the discovery of the excited bottom baryons but also it will provide possibility to study properties of heavy baryons as well as their electromagnetic, weak and strong decays.

Such an experimental progress stimulates the theoretical studies on properties of the heavy baryons as well as their electromagnetic, weak and strong transitions. The mass spectrum of the heavy baryons has been studied using various methods including heavy quark effective theory [2], QCD sum rules [3–6] and some other phenomenological models [7–12]. Some electromagnetic properties of the heavy baryons and their radiative decays have been investigated in different frameworks in [6, 13–24]. The strong decays of the heavy baryons have also been in the focus of much attention, theoretically (see for instance [25–27] and references therein).

However, the weak and semileptonic decays of heavy baryons are very important frameworks not only in obtaining information about their internal structure, precise calculation of the main ingredients of standard model (SM) such as Kabbibbo-Kobayashi-Maskawa (CKM) matrix elements and answering to some fundamental questions like nature of the CP violation, but also in looking for new physics beyond the SM. The loop level semileptonic transitions of the heavy baryons containing single heavy quark to light baryons induced by the flavor changing neutral currents (FCNC) are useful tools, for instance, to look for the supersymmetric particles, light dark matter, fourth generation of the quarks and extra dimensions etc. [28, 29]. Some semileptonic decay channels of the heavy baryons have been previously investigated in different frameworks (see for instance [30–38] and references therein).

The present work deals with the semileptonic decays of heavy $\Xi_{b(c)}$ and $\Xi'_{b(c)}$ baryons to the light Ξ and Σ baryons. The considered channels are either at loop level described by twelve form factors in full QCD or at tree level analyzed by six form factors entering the transition matrix elements of the corresponding low energy Hamiltonian. Here, we should mention that by the "full QCD" we refer to the QCD theory without any approximation like heavy quark effective theory (HQET) so we take the mass of heavy quarks finite. In HQET approximation, the number of form factors describing the considered transitions reduce to only two form factors [39, 40]. The considered processes take place in low energies far from the perturbative region, so to calculate the form factors as the main ingredients, we should consult some nonperturbative methods. One of the most powerful, applicable and attractive nonperturbative methods is QCD sum rules [41, 42] and its extension light cone sum rules (LCSR) (see for instance [43]). We apply the LCSR method to calculate the corresponding form factors in full theory. In this approach, the time ordering multiplication of the most general form of the interpolating currents for considered heavy baryons with transition currents are expanded in terms of the distribution amplitudes (DA's) of the light Ξ and Σ baryons. Using the obtained form factors, we calculate the decay rate and branching ratio for the considered channels.

The introduction is followed by section 2 which presents the details of the application of the LCSR method to find the QCD sum rules for the form factors. Section 3 is devoted to the numerical analysis of the form factors as well as evaluation of the decay widths and branching fractions. Finally, section 4 encompasses our conclusion.

2 LCSR for transition form factors

This section is dedicated to the details of calculations of the form factors. As we previously mentioned, the considered transitions can be classified as loop FCNC and tree level decays. The loop level transitions include the semileptonic $\Xi_b \to \Xi l^+ l^-$, $\Xi_b \to \Sigma l^+ l^-$, $\Xi_c \to \Sigma l^+ l^-$ $\Xi_b' \to \Xi l^+ l^-$, $\Xi_b' \to \Sigma l^+ l^-$ and $\Xi_c' \to \Sigma l^+ l^-$ decays. Considering the quark contents and charges of the participant baryons, these channels proceed via FCNC $b \to s$, $b \to d$ or $c \to u$ transitions at quark level. The low energy effective Hamiltonian describing the above transitions is written as:

$$\begin{aligned} \mathcal{H}_{eff}^{loop} = \frac{G_F \ \alpha_{em} V_{Q'Q} \ V_{Q'q}^{*}}{2\sqrt{2} \ \pi} \bigg\{ & C_9^{eff} \ \bar{q}\gamma_\mu(1-\gamma_5)Q\bar{l}\gamma^\mu l + C_{10} \ \bar{q}\gamma_\mu(1-\gamma_5)Q\bar{l}\gamma^\mu\gamma_5 l \\ & - 2m_Q \ C_7^{eff}\frac{1}{q^2} \ \bar{q}i\sigma_{\mu\nu}q^\nu(1+\gamma_5)Q\bar{l}\gamma^\mu l \bigg\} \ , \end{aligned} \tag{1}$$

where Q corresponds to b or c quark, Q' represents the t or b quark and q denotes the s, d or u quark with respect to the transition under consideration. The tree level transitions include the channels, $\Xi_c \to \Xi l\nu$, $\Xi_c \to \Sigma l\nu$, $\Xi_c' \to \Xi l\nu$ and $\Xi_c' \to \Sigma l\nu$, which proceed via $c \to s$ or $c \to d$ depending on the quark contents and charges of the initial and final baryons. The effective Hamiltonian representing the considered tree level transitions has the following form:

$$\mathcal{H}_{eff}^{tree} = \frac{G_F}{\sqrt{2}} V_{qc} \ \bar{q}\gamma_\mu(1-\gamma_5)c\bar{l}\gamma^\mu(1-\gamma_5)\nu, \tag{2}$$

where q can be either s or d quark, G_F is the Fermi coupling constant, and $V_{Q'Q}$, $V_{Q'q}$ and V_{qc} are elements of the CKM matrix.

In order to get the amplitudes, we need to sandwich the effective Hamiltonians between the initial and final states. Looking at the effective Hamiltonians, we see that we have two transition currents, $J_\mu^{tr,I} = \bar{q}\gamma_\mu(1-\gamma_5)Q$ and $J_\mu^{tr,II} = \bar{q}i\sigma_{\mu\nu}q^\nu(1-\gamma_5)Q$. The matrix elements of the transition currents are parameterized in terms of form factors in the following way:

$$\begin{aligned} \langle B(p) \mid J_\mu^{tr,I} \mid B_Q(p+q,s)\rangle = \bar{u}_B(p)\Big[& \gamma_\mu f_1(Q^2) + i\sigma_{\mu\nu}q^\nu f_2(Q^2) + q^\mu f_3(Q^2) \\ & - \gamma_\mu\gamma_5 g_1(Q^2) - i\sigma_{\mu\nu}\gamma_5 q^\nu g_2(Q^2) - q^\mu\gamma_5 g_3(Q^2)\Big] u_{B_Q}(p+q,s) \ , \end{aligned} \tag{3}$$

and

$$\begin{aligned} \langle B(p) \mid J_\mu^{tr,II} \mid B_Q(p+q,s)\rangle = \bar{u}_B(p)\Big[& \gamma_\mu f_1^T(Q^2) + i\sigma_{\mu\nu}q^\nu f_2^T(Q^2) + q^\mu f_3^T(Q^2) \\ & + \gamma_\mu\gamma_5 g_1^T(Q^2) + i\sigma_{\mu\nu}\gamma_5 q^\nu g_2^T(Q^2) + q^\mu\gamma_5 g_3^T(Q^2)\Big] u_{B_Q}(p+q,s) \ , \end{aligned} \tag{4}$$

where $Q^2 = -q^2$, f_i, g_i, f_i^T and g_i^T are transition form factors, and u_{B_Q} and u_B are spinors of the initial and final states. The $B_Q(p+q,s)$ stands for particles with momentum $p+q$ and spin s. From the explicit expressions of the effective Hamiltonians, it is clear that the loop level transitions contain both transition matrix elements having twelve form factors while the tree level channels include only the transition current I that corresponds to six form factors.

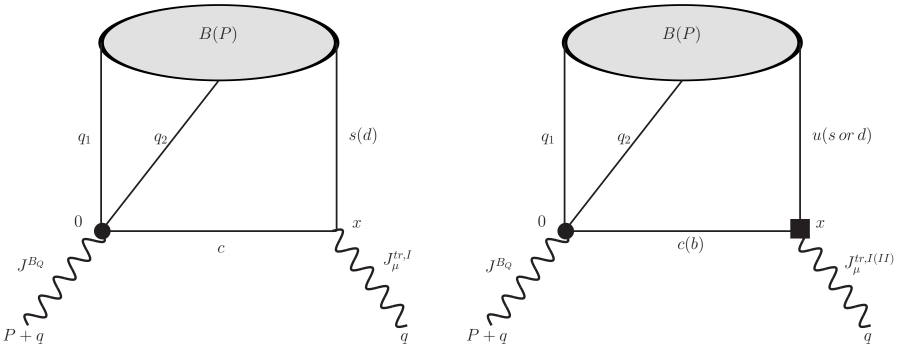

Figure 1: Diagrammatic representations of the correlation functions given in Eq. (5). The left (right) diagram belongs to the tree (loop) level transitions. The ovals (wavy lines) in diagrams stand for the DA's of Ξ or Σ baryons (external currents). In each graph, the q_1 and q_2 are light spectator quarks.

Our main task in the present work is to calculate the transition form factors. According to the philosophy of the QCD sum rules approach, we start with the following correlation functions as the main building blocks of the method:

$$\begin{aligned}
\Pi_\mu^{I}(p,q) &= i\int d^4x e^{iqx}\langle B(p) \mid T\{J_\mu^{tr,I}(x), \bar{J}^{B_Q}(0)\} \mid 0\rangle \ , \\
\Pi_\mu^{II}(p,q) &= i\int d^4x e^{iqx}\langle B(p) \mid T\{J_\mu^{tr,II}(x), \bar{J}^{B_Q}(0)\} \mid 0\rangle \ ,
\end{aligned} \tag{5}$$

where J^{B_Q} is the interpolating current carrying the quantum numbers of the $\Xi_Q(\Xi'_Q)$ baryons. The diagrammatic representations of these correlation functions are presented in Figure 1. The interpolating currents for the considered baryons have the following general forms (see for instance [44]):

$$\begin{aligned}
J^{\Xi'_Q} &= -\frac{1}{\sqrt{2}}\epsilon^{abc}\Big\{\Big(q_1^{aT}CQ^b\Big)\gamma_5 q_2^c + \beta\Big(q_1^{aT}C\gamma_5 Q^b\Big)q_2^c - \Big[\Big(Q^{aT}Cq_2^b\Big)\gamma_5 q_1^c + \beta\Big(Q^{aT}C\gamma_5 q_2^b\Big)q_1^c\Big]\Big\} \ , \\
J^{\Xi_Q} &= \frac{1}{\sqrt{6}}\epsilon^{abc}\Big\{2\Big(q_1^{aT}Cq_2^b\Big)\gamma_5 Q^c + 2\beta\Big(q_1^{aT}C\gamma_5 q_2^b\Big)Q^c + \Big(q_1^{aT}CQ^b\Big)\gamma_5 q_2^c + \beta\Big(q_1^{aT}C\gamma_5 Q^b\Big)q_2^c \\
&\quad + \Big(Q^{aT}Cq_2^b\Big)\gamma_5 q_1^c + \beta\Big(Q^{aT}C\gamma_5 q_2^b\Big)q_1^c\Big\} \ ,
\end{aligned} \tag{6}$$

where C is the charge conjugation operator, a, b and c are color indices and the light quarks q_1 and q_2 are given in Table 1. The β is an arbitrary parameter and the value $\beta = -1$ corresponds to the Ioffe current.

	$\Xi_{b(c)}^{-(0)}$	$\Xi_{b(c)}^{0(+)}$	$\Xi_{b(c)}^{\prime -(0)}$	$\Xi_{b(c)}^{\prime 0(+)}$
q_1	d	u	d	u
q_2	s	s	s	s

Table 1: The light quark contents of the heavy baryons Ξ_Q and Ξ'_Q.

The correlation functions given above can be calculated in two different ways. From the phenomenological or physical side, they are calculated inserting complete sets of hadronic states having the same quantum numbers as the chosen interpolating fields. The results of this side appear in terms of hadronic degrees of freedom. On the other side, the QCD or theoretical side of the correlation functions are calculated in terms of the B baryon DA's via operator product expansion (OPE). Then, we match these two different representations to relate the hadronic parameters to fundamental QCD degrees of freedom which leads to QCD sum rules for the considered form factors. To suppress contribution of the higher states and continuum, we apply Borel transformation with respect to the initial momentum squared to both sides of the sum rules and use the quark-hadron duality assumption.

Inserting complete set of hadronic state into correlation functions and isolating the contribution of the ground state, we obtain the following representations from physical side:

$$\Pi_\mu^I(p,q) = \sum_s \frac{\langle B(p) \mid J_\mu^{tr,I} \mid B_Q(p+q,s)\rangle\langle B_Q(p+q,s) \mid \bar{J}^{B_Q}(0) \mid 0\rangle}{m_{B_Q}^2-(p+q)^2} + \cdots\ , \tag{7}$$

$$\Pi_\mu^{II}(p,q) = \sum_s \frac{\langle B(p) \mid J_\mu^{tr,II} \mid B_Q(p+q,s)\rangle\langle B_Q(p+q,s) \mid \bar{J}^{B_Q}(0) \mid 0\rangle}{m_{B_Q}^2-(p+q)^2} + \cdots\ , \tag{8}$$

where the ... stands for the contributions of the higher states and continuum. To proceed, besides the transition matrix elements, we need also to know the matrix element $\langle B_Q(p+q,s) \mid \bar{J}^{B_Q}(0) \mid 0\rangle$ defined in terms of the residue λ_{B_Q},

$$\langle B_Q(p+q,s) \mid \bar{J}^{B_Q}(0) \mid 0\rangle = \lambda_{B_Q}\bar{u}_{B_Q}(p+q,s)\ . \tag{9}$$

Putting all definitions in Eqs. (7) and (8) and using the completeness relation for Dirac particle as

$$\sum_s u_{B_Q}(p+q,s)\overline{u}_{B_Q}(p+q,s) = \not{p} + \not{q} + m_{B_Q}\ , \tag{10}$$

we get the following final representations of the correlation functions in physical side:

$$\Pi_\mu^I(p,q) = \frac{\lambda_{B_Q}u_B(p)}{m_{B_Q}^2-(p+q)^2}\Big\{2f_1(Q^2)p_\mu + 2f_2(Q^2)p_\mu\not{q} + \Big[f_2(Q^2)+f_3(Q^2)\Big]q_\mu\not{q}$$
$$+\ 2g_1(Q^2)p_\mu\gamma_5 + 2g_2(Q^2)p_\mu\not{q}\gamma_5 + \Big[g_2(Q^2)+g_3(Q^2)\Big]q_\mu\not{q}\gamma_5$$

$$+ \text{ other structures}\Big\} + ... \ , \tag{11}$$

$$\begin{aligned}\Pi^{II}_{\mu}(p,q) = \frac{\lambda_{B_Q} u_B(p)}{m^2_{B_Q}-(p+q)^2}\Big\{ & 2f_1^T(Q^2)p_\mu + 2f_2^T(Q^2)p_\mu \not{q} + \Big[f_2^T(Q^2)+f_3^T(Q^2)\Big]q_\mu \not{q} \\ & - 2g_1^T(Q^2)p_\mu\gamma_5 - 2g_2^T(Q^2)p_\mu \not{q}\gamma_5 - \Big[g_2^T(Q^2)+g_3^T(Q^2)\Big]q_\mu \not{q}\gamma_5 \\ & + \text{ other structures}\Big\} + ... \ ,\end{aligned} \tag{12}$$

where we choose the represented structures to obtain sum rules for the form factors or their combinations. Here, we should comment that besides the presented structures, there are other structures which one can select to find the form factors. However, our calculations show that the selected structures lead to the more reliable results having good convergence of sum rules, i.e. in the coefficients of the selected structures, contribution of the higher twists is less than those of the lower twists.

Now, we turn our attention to calculate the QCD sides of the aforesaid correlation functions. They are calculated in deep Euclidean region, where $-(p+q)^2 \to \infty$. Using the explicit expressions of the interpolating currents and contracting out the quark pairs using the Wick's theorem, we find

$$\begin{aligned}\Pi^{I}_{\mu} &= \frac{i}{\sqrt{6}}\epsilon^{abc}\int d^4x e^{-iqx}\Big\{\Big(\Big[2(C)_{\phi\eta}(\gamma_5)_{\rho\beta}+(C)_{\phi\beta}(\gamma_5)_{\rho\eta}+(C)_{\beta\eta}(\gamma_5)_{\rho\phi}\Big]+\beta\Big[2(C\gamma_5)_{\phi\eta}(I)_{\rho\beta} \\ &+ (C\gamma_5)_{\phi\beta}(I)_{\rho\eta}+(C\gamma_5)_{\beta\eta}(I)_{\rho\phi}\Big]\Big)\Big[\gamma_\mu(1-\gamma_5)\Big]_{\sigma\theta}\Big\}S_b(-x)_{\beta\sigma}\langle 0|s^a_\eta(0)s^b_\theta(x)u^c_\phi(0)|\Xi(p)\rangle \ ,\end{aligned} \tag{13}$$

$$\begin{aligned}\Pi^{II}_{\mu} &= \frac{-i}{\sqrt{6}}\epsilon^{abc}\int d^4x e^{-iqx}\Big\{\Big(\Big[2(C)_{\phi\eta}(\gamma_5)_{\rho\beta}+(C)_{\phi\beta}(\gamma_5)_{\rho\eta}+(C)_{\beta\eta}(\gamma_5)_{\rho\phi}\Big]+\beta\Big[2(C\gamma_5)_{\phi\eta}(I)_{\rho\beta} \\ &+ (C\gamma_5)_{\phi\beta}(I)_{\rho\eta}+(C\gamma_5)_{\beta\eta}(I)_{\rho\phi}\Big]\Big)\Big[i\sigma_{\mu\nu}q^\nu(1-\gamma_5)\Big]_{\sigma\theta}\Big\}S_b(-x)_{\beta\sigma}\langle 0|s^a_\eta(0)s^b_\theta(x)u^c_\phi(0)|\Xi(p)\rangle \ ,\end{aligned} \tag{14}$$

for $\Xi_b \to \Xi l^+ l^-$,

$$\begin{aligned}\Pi^{I}_{\mu} &= \frac{i}{\sqrt{6}}\epsilon^{abc}\int d^4x e^{-iqx}\Big\{\Big(\Big[2(C)_{\phi\eta}(\gamma_5)_{\rho\beta}+(C)_{\phi\beta}(\gamma_5)_{\rho\eta}+(C)_{\beta\eta}(\gamma_5)_{\rho\phi}\Big]+\beta\Big[2(C\gamma_5)_{\phi\eta}(I)_{\rho\beta} \\ &+ (C\gamma_5)_{\phi\beta}(I)_{\rho\eta}+(C\gamma_5)_{\beta\eta}(I)_{\rho\phi}\Big]\Big)\Big[\gamma_\mu(1-\gamma_5)\Big]_{\sigma\theta}\Big\}S_b(-x)_{\beta\sigma}\langle 0|u^a_\eta(0)s^b_\theta(x)d^c_\phi(0)|\Sigma(p)\rangle \ ,\end{aligned} \tag{15}$$

$$\begin{aligned}\Pi^{II}_{\mu} &= \frac{-i}{\sqrt{6}}\epsilon^{abc}\int d^4x e^{-iqx}\Big\{\Big(\Big[2(C)_{\phi\eta}(\gamma_5)_{\rho\beta}+(C)_{\phi\beta}(\gamma_5)_{\rho\eta}+(C)_{\beta\eta}(\gamma_5)_{\rho\phi}\Big]+\beta\Big[2(C\gamma_5)_{\phi\eta}(I)_{\rho\beta} \\ &+ (C\gamma_5)_{\phi\beta}(I)_{\rho\eta}+(C\gamma_5)_{\beta\eta}(I)_{\rho\phi}\Big]\Big)\Big[i\sigma_{\mu\nu}q^\nu(1-\gamma_5)\Big]_{\sigma\theta}\Big\}S_b(-x)_{\beta\sigma}\langle 0|u^a_\eta(0)s^b_\theta(x)d^c_\phi(0)|\Sigma(p)\rangle \ ,\end{aligned} \tag{16}$$

for $\Xi_b \to \Sigma l^+ l^-$,

$$\begin{aligned}
\Pi_\mu^I &= \frac{i}{\sqrt{6}}\epsilon^{abc}\int d^4x e^{-iqx}\Bigg\{\Bigg(\Bigg(\Big[2(C)_{\phi\eta}(\gamma_5)_{\rho\beta}+(C)_{\phi\beta}(\gamma_5)_{\rho\eta}+(C)_{\beta\eta}(\gamma_5)_{\rho\phi}\Big]+\beta\Big[2(C\gamma_5)_{\phi\eta}(I)_{\rho\beta} \\
&+ (C\gamma_5)_{\phi\beta}(I)_{\rho\eta}+(C\gamma_5)_{\beta\eta}(I)_{\rho\phi}\Big]\Bigg)\Big[\gamma_\mu(1-\gamma_5)\Big]_{\sigma\theta}\Bigg\}S_b(-x)_{\beta\sigma}\langle 0|u_\eta^a(0)s_\theta^b(x)d_\phi^c(0)|\Sigma(p)\rangle\ ,
\end{aligned}\tag{17}$$

$$\begin{aligned}
\Pi_\mu^{II} &= \frac{-i}{\sqrt{6}}\epsilon^{abc}\int d^4x e^{-iqx}\Bigg\{\Bigg(\Bigg(\Big[2(C)_{\phi\eta}(\gamma_5)_{\rho\beta}+(C)_{\phi\beta}(\gamma_5)_{\rho\eta}+(C)_{\beta\eta}(\gamma_5)_{\rho\phi}\Big]+\beta\Big[2(C\gamma_5)_{\phi\eta}(I)_{\rho\beta} \\
&+ (C\gamma_5)_{\phi\beta}(I)_{\rho\eta}+(C\gamma_5)_{\beta\eta}(I)_{\rho\phi}\Big]\Big]\Bigg)\Big[i\sigma_{\mu\nu}q^\nu(1-\gamma_5)\Big]_{\sigma\theta}\Bigg\}S_b(-x)_{\beta\sigma}\langle 0|u_\eta^a(0)s_\theta^b(x)d_\phi^c(0)|\Sigma(p)\rangle\ ,
\end{aligned}\tag{18}$$

for $\Xi_c \to \Sigma l^+ l^-$,

$$\begin{aligned}
\Pi_\mu^I &= \frac{-i}{\sqrt{2}}\epsilon^{abc}\int d^4x e^{-iqx}\Bigg\{\Bigg(\Bigg(\Big[(C)_{\phi\beta}(\gamma_5)_{\rho\eta}-(C)_{\beta\eta}(\gamma_5)_{\rho\phi}\Big]+\beta\Big[(C\gamma_5)_{\phi\beta}(I)_{\rho\eta} \\
&- (C\gamma_5)_{\beta\eta}(I)_{\rho\phi}\Big]\Big]\Bigg)\Big[\gamma_\mu(1-\gamma_5)\Big]_{\sigma\theta}\Bigg\}S_b(-x)_{\beta\sigma}\langle 0|s_\eta^a(0)s_\theta^b(x)u_\phi^c(0)|\Xi(p)\rangle\ ,
\end{aligned}\tag{19}$$

$$\begin{aligned}
\Pi_\mu^{II} &= \frac{i}{\sqrt{2}}\epsilon^{abc}\int d^4x e^{-iqx}\Bigg\{\Bigg(\Bigg(\Big[(C)_{\phi\beta}(\gamma_5)_{\rho\eta}-(C)_{\beta\eta}(\gamma_5)_{\rho\phi}\Big]+\beta\Big[(C\gamma_5)_{\phi\beta}(I)_{\rho\eta} \\
&- (C\gamma_5)_{\beta\eta}(I)_{\rho\phi}\Big]\Big]\Bigg)\Big[i\sigma_{\mu\nu}q^\nu(1-\gamma_5)\Big]_{\sigma\theta}\Bigg\}S_b(-x)_{\beta\sigma}\langle 0|s_\eta^a(0)s_\theta^b(x)u_\phi^c(0)|\Xi(p)\rangle\ ,
\end{aligned}\tag{20}$$

for $\Xi_b' \to \Xi l^+ l^-$,

$$\begin{aligned}
\Pi_\mu^I &= \frac{-i}{\sqrt{2}}\epsilon^{abc}\int d^4x e^{-iqx}\Bigg\{\Bigg(\Bigg(\Big[(C)_{\phi\beta}(\gamma_5)_{\rho\eta}-(C)_{\beta\eta}(\gamma_5)_{\rho\phi}\Big]+\beta\Big[(C\gamma_5)_{\phi\beta}(I)_{\rho\eta} \\
&- (C\gamma_5)_{\beta\eta}(I)_{\rho\phi}\Big]\Big]\Bigg)\Big[\gamma_\mu(1-\gamma_5)\Big]_{\sigma\theta}\Bigg\}S_b(-x)_{\beta\sigma}\langle 0|d_\eta^a(0)s_\theta^b(x)d_\phi^c(0)|\Sigma(p)\rangle\ ,
\end{aligned}\tag{21}$$

$$\begin{aligned}
\Pi_\mu^{II} &= \frac{i}{\sqrt{2}}\epsilon^{abc}\int d^4x e^{-iqx}\Bigg\{\Bigg(\Bigg(\Big[(C)_{\phi\beta}(\gamma_5)_{\rho\eta}-(C)_{\beta\eta}(\gamma_5)_{\rho\phi}\Big]+\beta\Big[(C\gamma_5)_{\phi\beta}(I)_{\rho\eta} \\
&- (C\gamma_5)_{\beta\eta}(I)_{\rho\phi}\Big]\Big]\Bigg)\Big[i\sigma_{\mu\nu}q^\nu(1-\gamma_5)\Big]_{\sigma\theta}\Bigg\}S_b(-x)_{\beta\sigma}\langle 0|d_\eta^a(0)s_\theta^b(x)d_\phi^c(0)|\Sigma(p)\rangle\ ,
\end{aligned}\tag{22}$$

for $\Xi_b' \to \Sigma l^+ l^-$,

$$\begin{aligned}
\Pi_\mu^I &= \frac{-i}{\sqrt{2}}\epsilon^{abc}\int d^4x e^{-iqx}\Bigg\{\Bigg(\Bigg(\Big[(C)_{\phi\beta}(\gamma_5)_{\rho\eta}-(C)_{\beta\eta}(\gamma_5)_{\rho\phi}\Big]+\beta\Big[(C\gamma_5)_{\phi\beta}(I)_{\rho\eta}\\
&- (C\gamma_5)_{\beta\eta}(I)_{\rho\phi}\Big]\Bigg)\Big[\gamma_\mu(1-\gamma_5)\Big]_{\sigma\theta}\Bigg\}S_c(-x)_{\beta\sigma}\langle 0|u_\eta^a(0)s_\theta^b(x)d_\phi^c(0)|\Sigma(p)\rangle\ ,
\end{aligned} \tag{23}$$

$$\begin{aligned}
\Pi_\mu^{II} &= \frac{i}{\sqrt{2}}\epsilon^{abc}\int d^4x e^{-iqx}\Bigg\{\Bigg(\Bigg(\Big[(C)_{\phi\beta}(\gamma_5)_{\rho\eta}-(C)_{\beta\eta}(\gamma_5)_{\rho\phi}\Big]+\beta\Big[(C\gamma_5)_{\phi\beta}(I)_{\rho\eta}\\
&- (C\gamma_5)_{\beta\eta}(I)_{\rho\phi}\Big]\Bigg)\Big[i\sigma_{\mu\nu}q^\nu(1-\gamma_5)\Big]_{\sigma\theta}\Bigg\}S_c(-x)_{\beta\sigma}\langle 0|u_\eta^a(0)s_\theta^b(x)d_\phi^c(0)|\Sigma(p)\rangle\ ,
\end{aligned} \tag{24}$$

for $\Xi_c' \to \Sigma l^+ l^-$,

$$\begin{aligned}
\Pi_\mu &= \frac{i}{\sqrt{6}}\epsilon^{abc}\int d^4x e^{-iqx}\Bigg\{\Big[2(C)_{\phi\eta}(\gamma_5)_{\rho\beta}+(C)_{\phi\beta}(\gamma_5)_{\rho\eta}+(C)_{\beta\eta}(\gamma_5)_{\rho\phi}\Big]+\beta\Big[2(C\gamma_5)_{\phi\eta}(I)_{\rho\beta}\\
&+ (C\gamma_5)_{\phi\beta}(I)_{\rho\eta}+(C\gamma_5)_{\beta\eta}(I)_{\rho\phi}\Big]\Bigg\}\Big[\gamma_\mu(1-\gamma_5)\Big]_{\sigma\theta}S_c(-x)_{\beta\sigma}\langle 0|s_\eta^a(0)s_\theta^b(x)d_\phi^c(0)|\Xi(p)\rangle,
\end{aligned} \tag{25}$$

for $\Xi_c \to \Xi l\nu$,

$$\begin{aligned}
\Pi_\mu &= \frac{i}{\sqrt{6}}\epsilon^{abc}\int d^4x e^{-iqx}\Bigg\{\Big[2(C)_{\phi\eta}(\gamma_5)_{\rho\beta}+(C)_{\phi\beta}(\gamma_5)_{\rho\eta}+(C)_{\beta\eta}(\gamma_5)_{\rho\phi}\Big]+\beta\Big[2(C\gamma_5)_{\phi\eta}(I)_{\rho\beta}\\
&+ (C\gamma_5)_{\phi\beta}(I)_{\rho\eta}+(C\gamma_5)_{\beta\eta}(I)_{\rho\phi}\Big]\Bigg\}\Big[\gamma_\mu(1-\gamma_5)\Big]_{\sigma\theta}S_c(-x)_{\beta\sigma}\langle 0|u_\eta^a(0)s_\theta^b(x)d_\phi^c(0)|\Sigma(p)\rangle,
\end{aligned} \tag{26}$$

for $\Xi_c \to \Sigma l\nu$,

$$\begin{aligned}
\Pi_\mu &= \frac{-i}{\sqrt{2}}\epsilon^{abc}\int d^4x e^{-iqx}\Bigg\{\Big[(C)_{\phi\beta}(\gamma_5)_{\rho\eta}-(C)_{\beta\eta}(\gamma_5)_{\rho\phi}\Big]+\beta\Big[(C\gamma_5)_{\phi\beta}(I)_{\rho\eta}-(C\gamma_5)_{\beta\eta}(I)_{\rho\phi}\Big]\Bigg\}\\
&\Big[\gamma_\mu(1-\gamma_5)\Big]_{\sigma\theta}S_c(-x)_{\beta\sigma}\langle 0|s_\eta^a(0)s_\theta^b(x)u_\phi^c(0)|\Xi(p)\rangle,
\end{aligned} \tag{27}$$

for $\Xi_c' \to \Xi l\nu$, and

$$\begin{aligned}
\Pi_\mu &= \frac{-i}{\sqrt{2}}\epsilon^{abc}\int d^4x e^{-iqx}\Bigg\{\Big[(C)_{\phi\beta}(\gamma_5)_{\rho\eta}-(C)_{\beta\eta}(\gamma_5)_{\rho\phi}\Big]+\beta\Big[(C\gamma_5)_{\phi\beta}(I)_{\rho\eta}-(C\gamma_5)_{\beta\eta}(I)_{\rho\phi}\Big]\Bigg\}\\
&\Big[\gamma_\mu(1-\gamma_5)\Big]_{\sigma\theta}S_c(-x)_{\beta\sigma}\langle 0|u_\eta^a(0)s_\theta^b(x)d_\phi^c(0)|\Sigma(p)\rangle,
\end{aligned} \tag{28}$$

for $\Xi'_c \to \Sigma l \nu$, where $S_Q(x)$ is the heavy quark propagator which is given by [45]:

$$\begin{aligned} S_Q(x) &= S_Q^{free}(x) - i g_s \int \frac{d^4k}{(2\pi)^4} e^{-ikx} \int_0^1 dv \Bigg[\frac{\not{k} + m_Q}{(m_Q^2 - k^2)^2} G^{\mu\nu}(vx) \sigma_{\mu\nu} \\ &+ \frac{1}{m_Q^2 - k^2} v x_\mu G^{\mu\nu} \gamma_\nu \Bigg] , \end{aligned} \tag{29}$$

and,

$$S_Q^{free} = \frac{m_Q^2}{4\pi^2} \frac{K_1(m_b\sqrt{-x^2})}{\sqrt{-x^2}} - i \frac{m_Q^2 \not{x}}{4\pi^2 x^2} K_2(m_b\sqrt{-x^2}) , \tag{30}$$

with K_i being the Bessel functions. In Eq. (29), the S_Q^{free} corresponds to the free propagation of the heavy quark. The interaction of the heavy quark with the external gluon field is represented by the remaining terms. However calculation of these types of interactions requires knowledge of the currently unknown four-and five-particle baryonic DA's. The contribution of such terms are expected to be small [46–48], hence, in the present work we ignore their contributions.

To complete the calculations in QCD side, we need also the wave functions of the Ξ and Σ baryons, i.e., $\epsilon^{abc}\langle 0|s_\eta^a(0) s_\theta^b(x) u_\phi^c(0)|\Xi(p)\rangle$ and $\epsilon^{abc}\langle 0|u(d)_\eta^a(0) s_\theta^b(x) d_\phi^c(0)|\Sigma(p)\rangle$. These wave functions are expanded in terms of DA's having different twists which are calculated in [49] and [50]. For completeness, we present the explicit forms of the wave functions together with the DA's in the Appendix. Using the wave functions and heavy quark propagator we obtain the correlation functions in QCD side.

To obtain sum rules for the form factors, we match the coefficients of the same Dirac structures from both sides of the correlation functions. We also apply Borel transformation and continuum subtraction to suppress the contribution of the higher states and continuum. These processes bring us two auxiliary parameters, namely Borel mass parameter M^2 and continuum threshold s_0 which we will find the working regions for these quantities in the next section. In the meanwhile, we need also the residues $\lambda_{\Xi_Q(\Xi'_Q)}$ whose explicit forms are given in [24]. The explicit forms of sum rules for the form factors are very lengthy and we do not present their explicit expressions here, but we will give their fit functions in terms of q^2 in next section.

3 Numerical Results

In this section, we numerically analyze the form factors and obtain their behavior in terms of q^2. Using the fit functions of the form factors, we also calculate the decay rates for all considered channels and branching ratios for the channels in which the lifetime of initial particle is known. Some input parameters used in the numerical calculations are: $m_{\Xi_b^0} = (5790.5 \pm 2.7)$ MeV, $m_{\Xi'_b} = (5790.5 \pm 2.7)$ MeV, $m_{\Xi^0} = (1314.86 \pm 0.20)$ MeV, $m_{\Xi_c^0} = (2470.88^{+0.34}_{-0.80})$ MeV, $m_{\Xi_c'^+} = (2575.6 \pm 3.1)$ MeV, $m_{\Xi_c'^0} = (2577.9 \pm 2.9)$ MeV, $m_{\Sigma^0} = (1192.642 \pm 0.024)$ MeV, $m_{\Sigma^-} = (1197.449 \pm 0.030)$ MeV, $m_b = (4.7 \pm 0.1)$ GeV, $m_c = (1.27^{+0.07}_{-0.09})$ GeV, $|V_{cs}| = 1.023 \pm 0.036$, $|V_{cd}| = 0.230 \pm 0.011$, $|V_{tb}V_{td*}| = 8.27 \times 10^{-3}$,

$|V_{tb}V_{ts*}| = 0.041$, $V_{bc} = (41.2 \pm 1.1) \times 10^{-3}$, $V_{bu} = (3.93 \pm 0.36) \times 10^{-3}$ [1], $C_7^{eff} = -0.313$, $C_9^{eff} = 4.344$ and $C_{10} = -4.669$ [51].

The main input parameters of the LCSR for form factors are the DA's of the Ξ and Σ baryons presented in the Appendix. These DA's contain also four independent parameters. These parameters in the case of Ξ baryon are given as [49]:

$$\begin{aligned} f_\Xi &= (9.9 \pm 0.4) \times 10^{-3}\ \mathrm{GeV}^2, & \lambda_1 = -(2.8 \pm 0.1) \times 10^{-2}\ \mathrm{GeV}^2, \\ \lambda_2 &= (5.2 \pm 0.2) \times 10^{-2}\ \mathrm{GeV}^2, & \lambda_3 = (1.7 \pm 0.1) \times 10^{-2}\ \mathrm{GeV}^2, \end{aligned} \tag{31}$$

and for Σ baryon, they take the values [50]:

$$\begin{aligned} f_\Sigma &= (9.4 \pm 0.4) \times 10^{-3}\ \mathrm{GeV}^2, & \lambda_1 = -(2.5 \pm 0.1) \times 10^{-2}\ \mathrm{GeV}^2, \\ \lambda_2 &= (4.4 \pm 0.1) \times 10^{-2}\ \mathrm{GeV}^2, & \lambda_3 = (2.0 \pm 0.1) \times 10^{-2}\ \mathrm{GeV}^2. \end{aligned} \tag{32}$$

The LCSR for form factors contain also three auxiliary parameters. Borel mass parameter M^2 and continuum threshold s_0 are two of them coming from the Borel transformation and continuum subtraction, respectively. The general parameter β is the third parameter entering the calculations from the general form of the interpolating currents for B_Q baryons. According to the standard criteria in QCD sum rules, the results of form factors should be independent of these auxiliary parameters. Hence, we should look for working regions of these parameters such that the dependence of the results on these parameters are weak. The working region for the Borel mass parameter is determined requiring that not only the higher states and continuum contributions constitute a small percentage of the total dispersion integral but also the series of the light cone expansion with increasing twist should converge. This leads to the interval 15 $\mathrm{GeV}^2 \leq M^2 \leq 30\ \mathrm{GeV}^2$ for bottom baryons and 4 $\mathrm{GeV}^2 \leq M^2 \leq 10\ \mathrm{GeV}^2$ for charmed baryons. The continuum threshold s_0 is not totally arbitrary but it is related to the energy of the first excited state. Our numerical calculations show that in the region $(m_{B_Q} + 0.3)^2\ \mathrm{GeV}^2 \leq s_0 \leq (m_{B_Q} + 0.7)^2\ \mathrm{GeV}^2$, the results of the form factors exhibit very weak dependency on this parameter. Our numerical calculations also lead to the working region $-0.6 \leq \cos\theta \leq 0.3$ with $\tan\theta = \beta$ for the general parameter β. As an example, we present the dependence of the form factor f_2 for $\Xi_b \to \Xi\ell^+\ell^-$ on $\cos\theta$ and M^2 in Figures 2 and 3, respectively. From these figures, we see that the form factor f_2 depends weakly on the M^2 and s_0 compared to the $\cos\theta$. However, the dependence of the f_2 on $\cos\theta$ in the above mentioned working region is minimal compared to the intervals out of the working region.

Now, we proceed to find the q^2 dependence of the form factors in whole physical region, i.e. $4m_\ell^2 \leq q^2 \leq (m_{B_Q} - m_B)^2$ for loop level and $m_\ell^2 \leq q^2 \leq (m_{B_Q} - m_B)^2$ for tree level transitions. However, unfortunately the sum rules for form factors are truncated at some points and are not reliable in the whole physical region. This point for instance for the $\Xi_b \to \Xi l^+l^-$ transition is roughly at $q^2 = 15\ GeV^2$. To extend the results to whole physical region, we look for parametrization of the form factors such that in the reliable region, the results obtained from fit parametrization coincide with the sum rules predictions. Using the above working regions for the auxiliary parameters as well as other input parameters, we find that the form factors are well extrapolated by the fit parametrization,

$$f_i(q^2)[g_i(q^2)] = \frac{a}{(1 - \frac{q^2}{m_{fit}^2})} + \frac{b}{(1 - \frac{q^2}{m_{fit}^2})^2}. \tag{33}$$

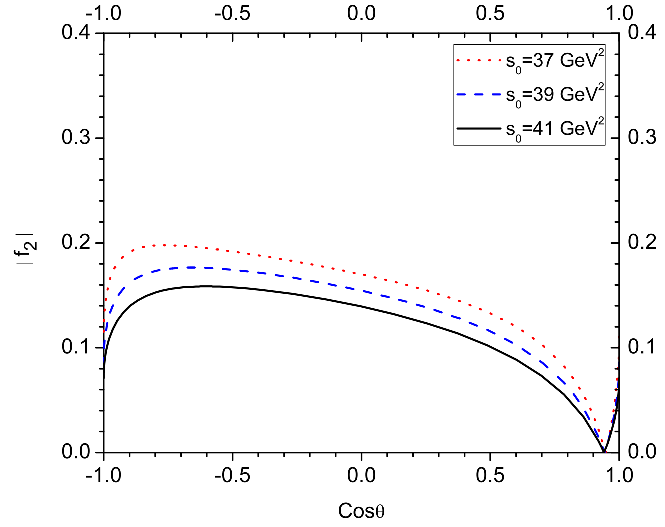

Figure 2: Form factor f_2 as a function of $\cos\theta$ for $\Xi_b \to \Xi \ell^+\ell^-$ decay at $q^2 = 13\ GeV^2$ and working region of M^2 .

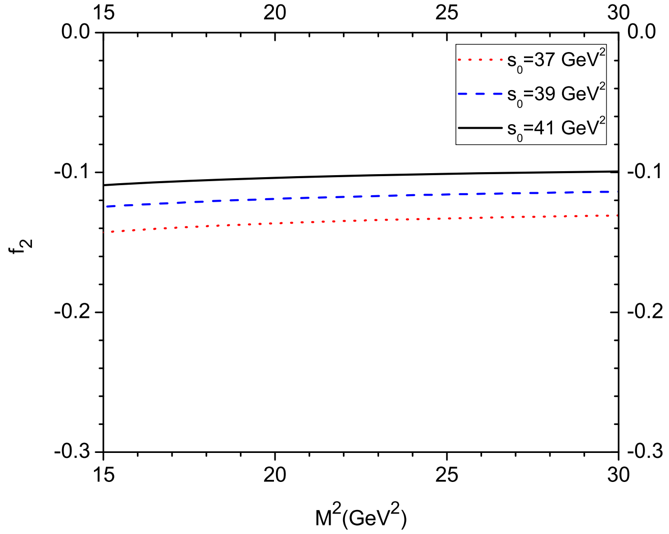

Figure 3: Form factor f_2 as a function of Borel mass parameter M^2 for $\Xi_b \to \Xi l^+ l^-$ decay at $q^2 = 13\ GeV^2$ and working region of β.

The central values for the fit parameters a, b, and m_{fit} as well as values of the form factors at $q^2 = 0$ are presented in Tables 7-16. The errors in the values of the form factors at $q^2 = 0$ are due to the variation of the auxiliary parameters M^2, s_0, and β in their working regions as well as the errors in the other input parameters. To see how the results obtained from the fit function coincide well with the sum rules predictions at reliable region, we depict the dependence of the form factors f_2 and f_2^T, as examples, on q^2 in figures 4 and 5. From these figures, we see that the results obtained from the fit parametrization describe well the sum rules results in the reliable region.

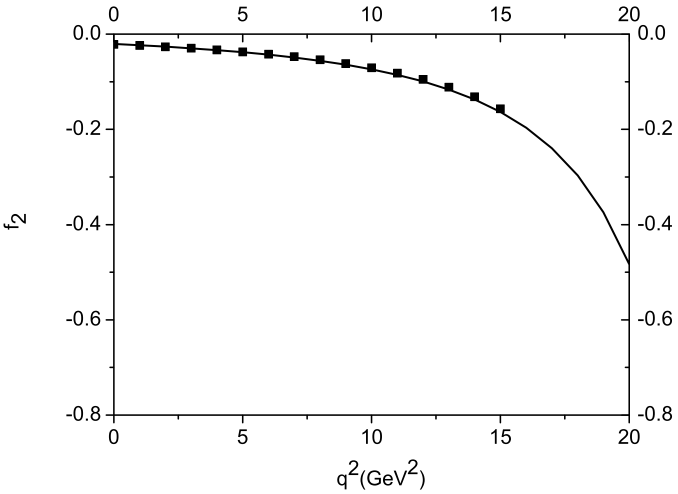

Figure 4: Form factor f_2 as a function of q^2 for $\Xi_b \to \Xi l^+ l^-$ decay at working regions of auxiliary parameters. The boxes show the sum rules predictions and the solid line belongs to the result obtained from fit parametrization.

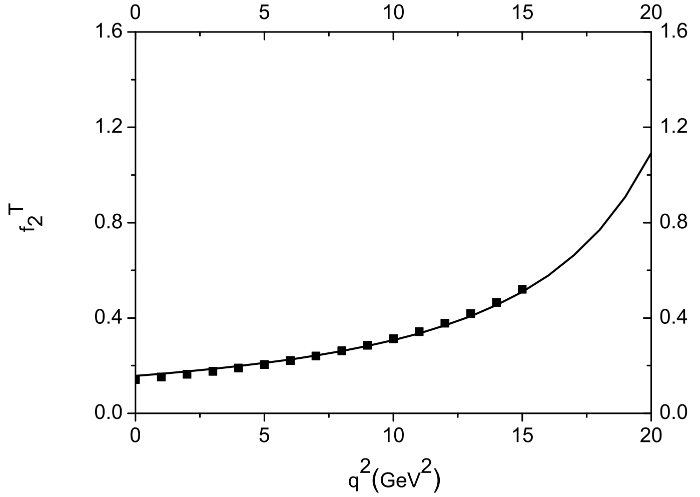

Figure 5: Form factor f_2^T as a function of q^2 for $\Xi_b \to \Xi l^+ l^-$ decay at working regions of auxiliary parameters. The boxes show the sum rules predictions and the solid line belongs to the result obtained from fit parametrization.

Our last task is to calculate the decay rates and branching ratios of the considered channels using the fit functions of the form factors. Considering the amplitudes of the transitions and definitions of the transition matrix elements in terms of form factors, the differential decay rate for loop level transitions is obtained as [37] :

$$\frac{d\Gamma}{ds} = \frac{G_F^2 \alpha_{em}^2 m_{B_Q}}{8192\pi^5} |V_{Q'Q} V_{Q'q}^*|^2 v\sqrt{\lambda} \left[\Theta(s) + \frac{1}{3}\Delta(s)\right] , \tag{34}$$

where $s = q^2/m_{B_Q}^2$, $G_F = 1.17 \times 10^{-5}$ GeV^{-2}, $\lambda = \lambda(1, r, s)$ with $\lambda(a, b, c) = a^2 + b^2 + c^2 - 2ab - 2ac - 2bc$ and $v = \sqrt{1 - \frac{4m_\ell^2}{q^2}}$ is the lepton velocity. The functions $\Theta(s)$ and $\Delta(s)$ are given as:

$$\begin{aligned}
\Theta(s) = {} & 32 m_\ell^2 m_{B_Q}^4 s(1+r-s)\left(|D_3|^2 + |E_3|^2\right) \\
& + 64 m_\ell^2 m_{B_Q}^3 (1-r-s)\,\mathrm{Re}[D_1^* E_3 + D_3 E_1^*] \\
& + 64 m_{B_Q}^2 \sqrt{r}(6m_\ell^2 - m_{B_Q}^2 s)\mathrm{Re}[D_1^* E_1] \\
& + 64 m_\ell^2 m_{B_Q}^3 \sqrt{r}\Big(2 m_{B_Q} s \mathrm{Re}[D_3^* E_3] + (1-r+s)\mathrm{Re}[D_1^* D_3 + E_1^* E_3]\Big) \\
& + 32 m_{B_Q}^2 (2m_\ell^2 + m_{B_Q}^2 s)\Big\{(1-r+s) m_{B_Q}\sqrt{r}\,\mathrm{Re}[A_1^* A_2 + B_1^* B_2] \\
& - m_{B_Q}(1-r-s)\,\mathrm{Re}[A_1^* B_2 + A_2^* B_1] - 2\sqrt{r}\Big(\mathrm{Re}[A_1^* B_1] + m_{B_Q}^2 s\,\mathrm{Re}[A_2^* B_2]\Big)\Big\} \\
& + 8 m_{B_Q}^2 \Big\{4m_\ell^2(1+r-s) + m_{B_Q}^2\Big[(1-r)^2 - s^2\Big]\Big\}\left(|A_1|^2 + |B_1|^2\right) \\
& + 8 m_{B_Q}^4 \Big\{4m_\ell^2\Big[\lambda + (1+r-s)s\Big] + m_{B_Q}^2 s\Big[(1-r)^2 - s^2\Big]\Big\}\left(|A_2|^2 + |B_2|^2\right) \\
& - 8 m_{B_Q}^2 \Big\{4m_\ell^2(1+r-s) - m_{B_Q}^2\Big[(1-r)^2 - s^2\Big]\Big\}\left(|D_1|^2 + |E_1|^2\right) \\
& + 8 m_{B_Q}^5 s v^2 \Big\{ - 8 m_{B_Q} s\sqrt{r}\,\mathrm{Re}[D_2^* E_2] + 4(1-r+s)\sqrt{r}\,\mathrm{Re}[D_1^* D_2 + E_1^* E_2] \\
& - 4(1-r-s)\,\mathrm{Re}[D_1^* E_2 + D_2^* E_1] + m_{B_Q}\Big[(1-r)^2 - s^2\Big]\left(|D_2|^2 + |E_2|^2\right)\Big\} ,
\end{aligned} \tag{35}$$

$$\begin{aligned}
\Delta(s) = {} & -8 m_{B_Q}^4 v^2 \lambda \left(|A_1|^2 + |B_1|^2 + |D_1|^2 + |E_1|^2\right) \\
& + 8 m_{B_Q}^6 s v^2 \lambda\Big(|A_2|^2 + |B_2|^2 + |D_2|^2 + |E_2|^2 \Big) ,
\end{aligned} \tag{36}$$

where $r = m_B^2/m_{B_Q}^2$ and

$$\begin{aligned}
A_1 &= \frac{1}{q^2}\left(f_1^T + g_1^T\right)\left(-2m_Q C_7\right) + \left(f_1 - g_1\right) C_9^{eff} \\
A_2 &= A_1\left(1 \to 2\right) , \\
A_3 &= A_1\left(1 \to 3\right) , \\
B_1 &= A_1\left(g_1 \to -g_1;\ g_1^T \to -g_1^T\right) , \\
B_2 &= B_1\left(1 \to 2\right) , \\
B_3 &= B_1\left(1 \to 3\right) , \\
D_1 &= \left(f_1 - g_1\right) C_{10} ,
\end{aligned}$$

$$
\begin{aligned}
D_2 &= D_1\,(1\to 2)\ , \\
D_3 &= D_1\,(1\to 3)\ , \\
E_1 &= D_1\,(g_1\to -g_1)\ , \\
E_2 &= E_1\,(1\to 2)\ , \\
E_3 &= E_1\,(1\to 3)\ .
\end{aligned} \tag{37}
$$

Integrating the differential decay rate over s in whole physical region, $4m_\ell^2/m_{B_Q}^2 \le s \le (1-\sqrt{r})^2$, one can obtain the total decay rate.

For the tree level transitions, the formula for the decay width is given by [52, 53]:

$$
\Gamma = \frac{G_F^2}{384\pi^3 m^3_{\Xi_c^{(\prime)}}}\,|V_{\rm cs(d)}|^2 \int\limits_{m_l^2}^{\delta^2} dq^2\ (1-m_l^2/q^2)^2\ \sqrt{(\sigma^2-q^2)(\delta^2-q^2)}\ N(q^2) \tag{38}
$$

where

$$
\begin{aligned}
N(q^2) \;=\;& F_1^2(q^2)(\delta^2(4q^2-m_l^2)+2\sigma^2\delta^2(1+2m_l^2/q^2)-(\sigma^2+2q^2)(2q^2+m_l^2)) \\
+\;& F_2^2(q^2)(\delta^2-q^2)(2\sigma^2+q^2)(2q^2+m_l^2)/m^2_{\Xi_c^{(\prime)}} + 3F_3^2(q^2)m_l^2(\sigma^2-q^2)q^2/m^2_{\Xi_c^{(\prime)}} \\
+\;& 6F_1(q^2)F_2(q^2)(\delta^2-q^2)(2q^2+m_l^2)\sigma/m_{\Xi_c^{(\prime)}} - 6F_1(q^2)F_3(q^2)m_l^2(\sigma^2-q^2)\delta/m_{\Xi_c^{(\prime)}} \\
+\;& G_1^2(q^2)(\sigma^2(4q^2-m_l^2)+2\sigma^2\delta^2(1+2m_l^2/q^2)-(\delta^2+2q^2)(2q^2+m_l^2)) \\
+\;& G_2^2(q^2)(\sigma^2-q^2)(2\delta^2+q^2)(2q^2+m_l^2)/m^2_{\Xi_c^{(\prime)}} + 3G_3^2(q^2)m_l^2(\delta^2-q^2)q^2/m^2_{\Xi_c^{(\prime)}} \\
-\;& 6G_1(q^2)G_2(q^2)(\sigma^2-q^2)(2q^2+m_l^2)\delta/m_{\Xi_c^{(\prime)}} + 6G_1(q^2)G_3(q^2)m_l^2(\delta^2-q^2)\sigma/m_{\Xi_c^{(\prime)}}\ ,
\end{aligned} \tag{39}
$$

with $F_1(q^2)=f_1(q^2)$, $F_2(q^2)=m_{\Xi_c^{(\prime)}}f_2(q^2)$, $F_3(q^2)=m_{\Xi_c^{(\prime)}}f_3(q^2)$, $G_1(q^2)=g_1(q^2)$, $G_2(q^2)=m_{\Xi_c^{(\prime)}}g_2(q^2)$, $G_3(q^2)=m_{\Xi_c^{(\prime)}}g_3(q^2)$, $\sigma=m_{\Xi_c^{(\prime)}}+m_B$, $\delta=m_{\Xi_c^{(\prime)}}-m_B$ and m_l is the lepton's mass. The numerical results of decay width for considered channels are presented in Table 17. Finally, for the channels which we know the lifetime of the initial particles [1], we calculate the branching ratios as presented in Table 18. The orders of branching fractions for most of the channels presented in Table 18 show that these channels are accessible at LHC.

4 Conclusion

In the present study, we have considered various loop level and tree level semileptonic decays of heavy $\Xi'_{b(c)}$ and $\Xi_{b(c)}$ baryons to the light Ξ and Σ baryons in the framework of the light cone QCD sum rules. The most general form of the interpolating currents for the considered heavy baryons as well as the recently available distribution amplitudes of the Ξ and Σ baryons have been used to calculate twelve form factors for loop level and six form factors for tree level transitions in full theory of QCD. Using the sum rules for the form factors, then, we have evaluated the decay rates of the related transitions. For those transitions with known lifetime, we have also calculated their branching fractions. The orders of branching fractions for tree level $\Xi_c \rightarrow \Sigma\ l^+\nu_l$ and $\Xi_c \rightarrow \Xi\ l^+\nu_l$ (with $l = e$ or μ) as well as rare loop level $\Xi_b \rightarrow \Xi\ l^+l^-$ and $\Xi_b \rightarrow \Sigma\ l^+l^-$ (with $l = e$ or μ or τ) transitions show that these channels can be detected at LHC. The similar baryonic $\Lambda_b \rightarrow \Lambda\ \mu^+\mu^-$ has been observed very recently by CDF Collaboration [54] and they reported the branching ratio of $[1.73 \pm 0.42(\text{stat}) \pm 0.55(\text{syst})] \times 10^{-6}$ which is in good consistency with our previous work [37]. Any measurement on the considered channels in the present work and comparison of the obtained data with our results can help us understand better the internal structures of the considered heavy baryons as well as obtain useful information about the distribution amplitudes of the Ξ and Σ baryons. Such comparison in FCNC channels can help us also in the course of searching for new physics effects beyond the SM.

5 Acknowledgment

Two of the authors (K. A. and H. S.) would like to thank TUBITAK, for their partial financial support provided under the project No.110T284.

References

[1] K. Nakamura *et al.*, J. Phys. G **37** , (2010) 075021.

[2] A. G. Grozin, O. I. Yakovlev, Phys. Lett. B **285** (1992) 254; Y. B. Dai, C. S. Huang, C. Liu, C. D. Lu, Phys. Lett. B **371** (1996) 99; D. W. Wang, M. Q. Huang, C. Z. Li, Phys. Rev. D **65** (2002) 094036.

[3] D. W. Wang, M. Q. Huang, Phys. Rev. D **68** (2003) 034019; Z. G. Wang, Eur. Phys. J. C **54** (2008) 231; F. O. Duraes, M. Nielsen, Phys. Lett. B **658** (2007) 40; X. Liu, H. X. Chen, Y. R. Liu, A. Hosaka, S. L. Zhu, Phys. Rev. D **77** (2008) 014031.

[4] E. V. Shuryak, Nucl. Phys. B **198** (1982) 83.

[5] Zhi-Gang Wang, Phys. Lett. B **685** (2010) 59.

[6] T. M. Aliev, K. Azizi, A. Ozpineci, Nucl. Phys. B **808**, (2009) 137.

[7] M. Karliner, H. J. Lipkin, Phys. Lett. B **660** (2008) 539.

[8] M. Karliner, B. Kereu-Zura, H. J. Lipkin, J. L. Rosner, arXiv:0706.2163 [hep-ph].

[9] D. Ebert, R. N. Faustov, V. O. Galkin, Phys. Rev. D **72** (2005) 034026.

[10] N. Mathur, R. Lewis , R. M. Woloshyn, Phys. Rev. D **66** (2002) 014502.

[11] J. L. Rosner, Phys. Rev. D **75** (2007) 013009.

[12] Qiao-Yan Zhao, Dan Zhang, Qiu-Yang Zhang, Chin. Phys. Lett. **28**, (2011) 071201.

[13] A. L. Choudhury, V. Joshi, Phys. Rev. D **13** (1976) 3115.

[14] D. B. Lichtenberg, Phys. Rev. D **15** (1977) 345.

[15] R. J. Johnson, M. Shah-Jahan, Phys. Rev. D **15** (1977) 1400.

[16] S. K. Bose, L. P. Singh, Phys. Rev. D **22** (1980) 773.

[17] L. Y. Glozman, D. O. Riska, Nucl. Phys. A **603** (1996) 326.

[18] B. Julia-Diaz, D. O. Riska, Nucl. Phys. A **739** (2004) 69.

[19] S. Scholl, H. Weigel, Nucl. Phys. A **735** (2004) 163.

[20] Y. S. Oh, B. Y. Park, Mod. Phys. Lett. A **11** (1996) 653.

[21] A. Faessler et. al, Phys. Rev. D **73** (2006) 094013.

[22] S. L. Zhu, W. Y. Hwang, Z. S. Yang, Phys. Rev. D **56** (1997) 7273.

[23] T. M. Aliev, K. Azizi, A. Ozpineci, Phys. Rev. D **77** (2008) 114006.

[24] T. M. Aliev, K. Azizi, A. Ozpineci, Phys. Rev. D **79**, (2009) 056005.

[25] T. M. Aliev, K. Azizi, M. Savci, Phys. Lett. B **696** (2011) 220.

[26] T. M. Aliev, K. Azizi, M. Savci, Nucl. Phys. A **852** (2011) 141

[27] T. M. Aliev, K. Azizi, M. Savci, V. S. Zamiralov, Phys. Rev. D **83**, (2011) 096007.

[28] G. Buchalla, G. Hiller and G. Isidori, Phys. Rev. D **63** (2000) 014015.

[29] C. Bird, P. Jackson, R. Kowalewski, M. Pospelov, Phys. Rev. Lett. **93** (2004) 201803.

[30] D. Ebert, R. N. Faustov, and V. O. Galkin, Phys. Rev. D **73**, (2006) 094002.

[31] Ming-Qiu Huang, Dao-Wei Wang, Phys. Rev. D **69**, (2004) 094003; arXiv:0608170v2 (hep-ph).

[32] C. Albertus, E. Hernandez, and J. Nieves, Phys. Rev. D **71**, (2005) 014012.

[33] Ruben Flores-Mendieta, J.J. Torres, M. Neri, A. Martinez, A. Garcia, Phys. Rev. D **71**, (2005) 034023.

[34] Muslema Pervin, Winston Roberts, and Simon Capstick, Phys. Rev. C **72**, (2005) 035201.

[35] K. Azizi, M. Bayar, A. Ozpineci, Y. Sarac, Phys. Rev. D **80**, (2009) 036007.

[36] K. Azizi, M. Bayar, Y. Sarac, H. Sundu, Phys. Rev. D **80**, (2009) 096007.

[37] T. M. Aliev, K. Azizi, M. Savci, Phys. Rev. D **81**, (2010) 056006.

[38] K. Azizi, M. Bayar, M. T. Zeyrek, J. Phys. G: Nucl. Part. Phys. **37**, (2010) 085002.

[39] T. Mannel, W. Roberts and Z. Ryzak, Nucl. Phys. B **355** (1991) 38.

[40] T. M. Aliev, A. Ozpineci, M. Savci, Phys. Rev. D **65** (2002) 115002.

[41] M. A. Shifman, A. I. Vainshtein and V. I. Zakharov, Nucl. Phys. B **147**, 385 (1979).

[42] M. A. Shifman, A. I. Vainstein, V. I. Zakharov, Nucl. Phys. B **147**, 448 (1979).

[43] I. I. Balitsky, V. M. Braun, A. V. Kolesnichenko, Nucl. Phys. B **312** (1989) 509.

[44] E. Bagan, M. Chabab, H. G. Dosch, S. Narison, Phys. Lett. B **278**, (1992) 369.

[45] I. I. Balitsky, V. M. Braun, Nucl. Phys. B **311** (1989) 541.

[46] V. M. Braun, A. Lenz, M. Wittmann, Phys. Rev. D **73** (2006) 094019.

[47] V. M. Braun, A. Lenz, N. Mahnke, E. Stein, Phys. Rev. D **65** (2002) 074011; A. Lenz, M. Wittmann and E. Stein, Phys. Lett. B **581**, 199 (2004).

[48] V. Braun, R. J. Fries, N. Mahnke and E. Stein, Nucl. Phys. B **589** (2000) 381.

[49] Yong-Lu Liu, Ming-Qiu Huang, Phys. Rev. D **80**, (2009) 055015.

[50] Y. L. Liu, M. Q. Huang, Nucl. Phys. A **821**, (2009) 80.

[51] A. J. Buras, M. Muenz Phys. Rev. D**52** (1995) 186.

[52] A. Faessler, T. Gutsche, B. R. Holstein, M. A. Ivanov, J. G. Korner, V. E. Lyubovitskij, Phys. Rev. D **78**, (2008) 094005.

[53] H. Pietschmann, Acta Phys. Austriaca Suppl. **12**, (1974) 1.

[54] T. Aaltonen et al. (CDF Collaboration), Phys. Rev. Lett. **107**, 201802 (2011).

Appendix A

In this Appendix, we present the general decomposition of the wave functions of the baryons in final states, i.e., $\epsilon^{abc}\langle 0|{q_1}_\eta^a(0){q_2}_\theta^b(x){q_3}_\phi^c(0)|B(p)\rangle$ and DA's of the Ξ and Σ baryons [49, 50]:

$$\begin{aligned}
& 4\langle 0|\epsilon^{abc}{q_1}_\alpha^a(a_1x){q_2}_\beta^b(a_2x){q_3}_\gamma^c(a_3x)|B(p)\rangle \\
&= \mathcal{S}_1 m_B C_{\alpha\beta}(\gamma_5 B)_\gamma + \mathcal{S}_2 m_B^2 C_{\alpha\beta}(\not{x}\gamma_5 B)_\gamma \\
&+ \mathcal{P}_1 m_B(\gamma_5 C)_{\alpha\beta}B_\gamma + \mathcal{P}_2 m_B^2(\gamma_5 C)_{\alpha\beta}(\not{x}B)_\gamma + (\mathcal{V}_1 + \frac{x^2m_B^2}{4}\mathcal{V}_1^M)(\not{p}C)_{\alpha\beta}(\gamma_5 B)_\gamma \\
&+ \mathcal{V}_2 m_B(\not{p}C)_{\alpha\beta}(\not{x}\gamma_5 B)_\gamma + \mathcal{V}_3 m_B(\gamma_\mu C)_{\alpha\beta}(\gamma^\mu\gamma_5 B)_\gamma + \mathcal{V}_4 m_B^2(\not{x}C)_{\alpha\beta}(\gamma_5 B)_\gamma \\
&+ \mathcal{V}_5 m_B^2(\gamma_\mu C)_{\alpha\beta}(i\sigma^{\mu\nu}x_\nu\gamma_5 B)_\gamma + \mathcal{V}_6 m_B^3(\not{x}C)_{\alpha\beta}(\not{x}\gamma_5 B)_\gamma + (\mathcal{A}_1 \\
&+ \frac{x^2m_B^2}{4}\mathcal{A}_1^M)(\not{p}\gamma_5 C)_{\alpha\beta}B_\gamma + \mathcal{A}_2 m_B(\not{p}\gamma_5 C)_{\alpha\beta}(\not{x}B)_\gamma + \mathcal{A}_3 m_B(\gamma_\mu\gamma_5 C)_{\alpha\beta}(\gamma^\mu B)_\gamma \\
&+ \mathcal{A}_4 m_B^2(\not{x}\gamma_5 C)_{\alpha\beta}B_\gamma + \mathcal{A}_5 m_B^2(\gamma_\mu\gamma_5 C)_{\alpha\beta}(i\sigma^{\mu\nu}x_\nu B)_\gamma + \mathcal{A}_6 m_B^3(\not{x}\gamma_5 C)_{\alpha\beta}(\not{x}B)_\gamma \\
&+ (\mathcal{T}_1 + \frac{x^2m_B^2}{4}\mathcal{T}_1^M)(p^\nu i\sigma_{\mu\nu}C)_{\alpha\beta}(\gamma^\mu\gamma_5 B)_\gamma + \mathcal{T}_2 m_B(x^\mu p^\nu i\sigma_{\mu\nu}C)_{\alpha\beta}(\gamma_5 B)_\gamma \\
&+ \mathcal{T}_3 m_B(\sigma_{\mu\nu}C)_{\alpha\beta}(\sigma^{\mu\nu}\gamma_5 B)_\gamma + \mathcal{T}_4 m_B(p^\nu\sigma_{\mu\nu}C)_{\alpha\beta}(\sigma^{\mu\rho}x_\rho\gamma_5 B)_\gamma \\
&+ \mathcal{T}_5 m_B^2(x^\nu i\sigma_{\mu\nu}C)_{\alpha\beta}(\gamma^\mu\gamma_5 B)_\gamma + \mathcal{T}_6 m_B^2(x^\mu p^\nu i\sigma_{\mu\nu}C)_{\alpha\beta}(\not{x}\gamma_5 B)_\gamma \\
&+ \mathcal{T}_7 m_B^2(\sigma_{\mu\nu}C)_{\alpha\beta}(\sigma^{\mu\nu}\not{x}\gamma_5 B)_\gamma + \mathcal{T}_8 m_B^3(x^\nu\sigma_{\mu\nu}C)_{\alpha\beta}(\sigma^{\mu\rho}x_\rho\gamma_5 B)_\gamma \ . \qquad (A.1)
\end{aligned}$$

The calligraphic functions in the above expression have not definite twists but they can be written in terms of the B distribution amplitudes (DA's) with definite and increasing twists via the scalar product px. The relationship between the calligraphic functions appearing in the above equation and scalar, pseudo-scalar, vector, axial vector and tensor DA's for B baryon are given in Tables 2, 3, 4, 5 and 6, respectively.

$\mathcal{S}_1 = S_1$
$2px\mathcal{S}_2 = S_1 - S_2$

Table 2: Relations between the calligraphic functions and B scalar DA's.

$\mathcal{P}_1 = P_1$
$2px\mathcal{P}_2 = P_1 - P_2$

Table 3: Relations between the calligraphic functions and B pseudo-scalar DA's.

Every distribution amplitude, $F= S_{1,2},\ P_{1,2},\ V_{1\to6},\ A_{1\to6},\ T_{1\to8}$ can be represented as:

$$F(a_ipx) = \int dx_1dx_2dx_3\delta(x_1+x_2+x_3-1)e^{-ipx(\sum_{j=1}^3 x_ja_j)}F(x_i) \ . \qquad (A.2)$$

where, x_i with $i = 1,\ 2$ or 3 are longitudinal momentum fractions carried by the participating quarks.

$\mathcal{V}_1 = V_1$
$2px\mathcal{V}_2 = V_1 - V_2 - V_3$
$2\mathcal{V}_3 = V_3$
$4px\mathcal{V}_4 = -2V_1 + V_3 + V_4 + 2V_5$
$4px\mathcal{V}_5 = V_4 - V_3$
$4(px)^2\mathcal{V}_6 = -V_1 + V_2 + V_3 + V_4 + V_5 - V_6$

Table 4: Relations between the calligraphic functions and B vector DA's.

$\mathcal{A}_1 = A_1$
$2px\mathcal{A}_2 = -A_1 + A_2 - A_3$
$2\mathcal{A}_3 = A_3$
$4px\mathcal{A}_4 = -2A_1 - A_3 - A_4 + 2A_5$
$4px\mathcal{A}_5 = A_3 - A_4$
$4(px)^2\mathcal{A}_6 = A_1 - A_2 + A_3 + A_4 - A_5 + A_6$

Table 5: Relations between the calligraphic functions and B axial vector DA's.

The explicit expressions for the DA's of the B baryon up to twists six are given as [49, 50]:

Twist-3 distribution amplitudes:

$$\begin{aligned} V_1(x_i) &= 120x_1x_2x_3\phi_3^0\,, \qquad\qquad A_1(x_i) = 0\,, \\ T_1(x_i) &= 120x_1x_2x_3\phi_3^{\prime 0}\,. \end{aligned} \tag{40}$$

Twist-4 distribution amplitudes:

$$\begin{aligned} S_1(x_i) &= 6(x_2 - x_1)x_3(\xi_4^0 + \xi_4^{\prime 0})\,, \qquad P_1(x_i) = 6(x_2 - x_1)x_3(\xi_4^0 - \xi_4^{\prime 0})\,, \\ V_2(x_i) &= 24x_1x_2\phi_4^0\,, \qquad A_2(x_i) = 0\,, \\ V_3(x_i) &= 12x_3(1 - x_3)\psi_4^0\,, \qquad A_3(x_i) = -12x_3(x_1 - x_2)\psi_4^0\,, \\ T_2(x_i) &= 24x_1x_2\phi_4^{\prime 0}\,, \qquad T_3(x_i) = 6x_3(1 - x_3)(\xi_4^0 + \xi_4^{\prime 0})\,, \\ T_7(x_i) &= 6x_3(1 - x_3)(\xi_4^{\prime 0} - \xi_4^0)\,. \end{aligned} \tag{41}$$

Twist-5 distribution amplitudes:

$$\begin{aligned} S_2(x_i) &= \frac{3}{2}(x_1 - x_2)(\xi_5^0 + \xi_5^{\prime 0})\,, \qquad P_2(x_i) = \frac{3}{2}(x_1 - x_2)(\xi_5^0 - \xi_5^{\prime 0})\,, \\ V_4(x_i) &= 3(1 - x_3)\psi_5^0\,, \qquad A_4(x_i) = 3(x_1 - x_2)\psi_5^0\,, \\ V_5(x_i) &= 6x_3\phi_5^0\,, \qquad A_5(x_i) = 0\,, \\ T_4(x_i) &= -\frac{3}{2}(x_1 + x_2)(\xi_5^{\prime 0} + \xi_5^0)\,, \qquad T_5(x_i) = 6x_3\phi_5^{\prime 0}\,, \\ T_8(x_i) &= \frac{3}{2}(x_1 + x_2)(\xi_5^{\prime 0} - \xi_5^0)\,. \end{aligned} \tag{42}$$

Twist-6 distribution amplitudes:

$$\begin{aligned} V_6(x_i) &= 2\phi_6^0\,, \qquad A_6(x_i) = 0\,, \\ T_6(x_i) &= 2\phi_6^{\prime 0}\,. \end{aligned} \tag{43}$$

$\mathcal{T}_1 = T_1$
$2px\mathcal{T}_2 = T_1 + T_2 - 2T_3$
$2\mathcal{T}_3 = T_7$
$2px\mathcal{T}_4 = T_1 - T_2 - 2T_7$
$2px\mathcal{T}_5 = -T_1 + T_5 + 2T_8$
$4(px)^2\mathcal{T}_6 = 2T_2 - 2T_3 - 2T_4 + 2T_5 + 2T_7 + 2T_8$
$4px\mathcal{T}_7 = T_7 - T_8$
$4(px)^2\mathcal{T}_8 = -T_1 + T_2 + T_5 - T_6 + 2T_7 + 2T_8$

Table 6: Relations between the calligraphic functions and B tensor DA's.

where,

$$\begin{aligned}
\phi_3^0 &= \phi_6^0 = f_B, \qquad\qquad \psi_4^0 = \psi_5^0 = \frac{1}{2}(f_B - \lambda_1)\,, \\
\phi_4^0 &= \phi_5^0 = \frac{1}{2}(f_B + \lambda_1), \qquad \phi_3'^0 = \phi_6'^0 = -\xi_5^0 = \frac{1}{6}(4\lambda_3 - \lambda_2)\,, \\
\phi_4'^0 &= \xi_4^0 = \frac{1}{6}(8\lambda_3 - 3\lambda_2), \qquad \phi_5'^0 = -\xi_5'^0 = \frac{1}{6}\lambda_2\,, \\
\xi_4'^0 &= \frac{1}{6}(12\lambda_3 - 5\lambda_2)\,. \qquad (44)
\end{aligned}$$

	a	b	m_{fit}	$q^2 = 0$
f_1	0.166	-0.024	5.35	0.142 ± 0.036
f_2	0.028	-0.048	5.31	-0.020 ± 0.005
f_3	-0.004	-0.006	5.37	-0.010 ± 0.002
g_1	0.106	0.054	5.24	0.160 ± 0.042
g_2	-0.005	-0.004	5.28	-0.009 ± 0.002
g_3	0.003	-0.006	4.70	-0.003 ± 0.001
f_1^T	0.127	-0.129	5.10	-0.0020 ± 0.0005
f_2^T	0.072	0.085	5.40	0.157 ± 0.041
f_3^T	-0.003	0.049	5.23	0.046 ± 0.011
g_1^T	0.288	-0.312	4.80	-0.024 ± 0.006
g_2^T	0.036	0.119	4.70	0.155 ± 0.040
g_3^T	0.024	-0.095	5.33	-0.071 ± 0.018

Table 7: Parameters appearing in the fit function of the form factors and the values of the form factors at $q^2 = 0$ for $\Xi_b \to \Xi \ell^+ \ell^-$.

	a	b	m_{fit}	$q^2 = 0$
f_1	0.035	0.011	5.16	0.046 ± 0.011
f_2	0.027	−0.060	5.32	-0.033 ± 0.008
f_3	0.086	−0.110	5.38	-0.024 ± 0.006
g_1	0.047	0.020	5.34	0.067 ± 0.017
g_2	−0.003	−0.021	5.25	-0.024 ± 0.006
g_3	−0.003	−0.024	5.39	-0.027 ± 0.006
f_1^T	0.045	−0.047	5.29	-0.0020 ± 0.0005
f_2^T	0.034	0.015	5.25	0.049 ± 0.012
f_3^T	−0.145	0.168	5.17	0.023 ± 0.006
g_1^T	0.006	−0.012	4.67	-0.006 ± 0.001
g_2^T	−0.041	0.054	5.38	0.013 ± 0.003
g_3^T	0.049	−0.071	5.36	-0.022 ± 0.005

Table 8: Parameters appearing in the fit function of the form factors and the values of the form factors at $q^2 = 0$ for $\Xi_b \to \Sigma \ell^+ \ell^-$.

	a	b	m_{fit}	$q^2 = 0$
f_1	0.526	-0.116	1.53	0.409 ± 0.106
f_2	-0.550	0.026	1.58	-0.524 ± 0.136
f_3	-0.204	-0.582	1.57	-0.786 ± 0.204
g_1	0.183	0.154	1.55	0.337 ± 0.088
g_2	-0.431	0.045	1.63	-0.386 ± 0.100
g_3	-0.190	-0.285	1.63	-0.475 ± 0.123
f_1^T	0.042	-0.048	1.56	-0.006 ± 0.001
f_2^T	0.585	-0.125	1.52	0.460 ± 0.120
f_3^T	-0.449	1.127	1.59	0.678 ± 0.176
g_1^T	0.058	-0.062	1.58	-0.004 ± 0.001
g_2^T	0.730	-0.201	1.57	0.529 ± 0.260
g_3^T	-0.531	-0.148	1.61	-0.679 ± 0.176

Table 9: Parameters appearing in the fit function of the form factors and the values of the form factors at $q^2 = 0$ for $\Xi_c \to \Sigma \ell^+ \ell^-$.

	a	b	m_{fit}	$q^2 = 0$
f_1	0.092	-0.003	5.30	0.089 ± 0.022
f_2	-0.010	-0.021	5.32	-0.031 ± 0.007
f_3	0.015	-0.058	5.73	-0.043 ± 0.010
g_1	-0.421	0.477	5.20	0.056 ± 0.014
g_2	-0.012	-0.008	5.10	-0.020 ± 0.005
g_3	-0.035	0.001	5.00	-0.034 ± 0.008
f_1^T	-1.126	1.124	5.40	-0.0020 ± 0.0005
f_2^T	0.028	0.081	4.80	0.109 ± 0.028
f_3^T	0.035	0.132	5.26	0.167 ± 0.043
g_1^T	0.645	-0.645	5.40	0.000 ± 0.000
g_2^T	0.022	0.002	4.80	0.024 ± 0.006
g_3^T	-0.210	-0.058	5.32	-0.268 ± 0.070

Table 10: Parameters appearing in the fit function of the form factors and the values of the form factors at $q^2 = 0$ for $\Xi_b' \to \Xi \ell^+ \ell^-$.

	a	b	m_{fit}	$q^2 = 0$
f_1	0.034	0.056	5.13	0.090 ± 0.022
f_2	0.046	-0.104	5.34	-0.058 ± 0.014
f_3	0.055	-0.104	5.27	-0.049 ± 0.012
g_1	-0.237	0.275	5.36	0.038 ± 0.010
g_2	0.008	-0.049	5.34	-0.041 ± 0.011
g_3	-0.006	-0.039	5.31	-0.045 ± 0.011
f_1^T	0.458	-0.458	5.15	0.000 ± 0.000
f_2^T	-0.541	0.679	5.35	0.138 ± 0.036
f_3^T	-0.281	0.494	5.38	0.213 ± 0.055
g_1^T	0.722	-0.725	5.08	-0.003 ± 0.001
g_2^T	-0.106	0.191	5.28	0.085 ± 0.021
g_3^T	0.025	-0.327	5.32	-0.302 ± 0.078

Table 11: Parameters appearing in the fit function of the form factors and the values of the form factors at $q^2 = 0$ for $\Xi_b^{'} \to \Sigma \ell^+ \ell^-$.

	a	b	m_{fit}	$q^2 = 0$
f_1	-0.564	0.640	1.52	0.076 ± 0.019
f_2	-0.426	-0.258	1.55	-0.684 ± 0.178
f_3	-0.642	-0.297	1.58	-0.939 ± 0.244
g_1	-0.092	0.212	1.62	0.120 ± 0.031
g_2	-0.265	-0.081	1.60	-0.346 ± 0.090
g_3	0.238	-0.349	1.55	-0.111 ± 0.029
f_1^T	0.272	-0.293	1.60	-0.021 ± 0.005
f_2^T	0.432	0.112	1.53	0.544 ± 0.141
f_3^T	-0.433	0.605	1.62	0.172 ± 0.045
g_1^T	0.258	-0.265	1.72	-0.007 ± 0.002
g_2^T	0.401	-0.013	1.50	0.388 ± 0.101
g_3^T	0.153	-0.510	1.63	-0.357 ± 0.093

Table 12: Parameters appearing in the fit function of the form factors and the values of the form factors at $q^2 = 0$ for $\Xi_c^{'} \to \Sigma \ell^+ \ell^-$.

	a	b	m_{fit}	$q^2 = 0$
f_1	-0.4142	0.608	1.52	0.194 ± 0.050
f_2	-0.320	-0.036	1.60	-0.356 ± 0.092
f_3	1.068	-1.530	1.55	-0.462 ± 0.120
g_1	-0.624	0.935	1.58	0.311 ± 0.081
g_2	0.010	-0.161	1.63	-0.151 ± 0.038
g_3	1.398	-1.710	1.61	-0.312 ± 0.081

Table 13: Parameters appearing in the fit function of the form factors and the values of the form factors at $q^2 = 0$ for $\Xi_c \to \Xi \ell \nu$.

	a	b	m_{fit}	$q^2 = 0$
f_1	0.528	-0.119	1.52	0.409 ± 0.106
f_2	-0.564	0.006	1.58	-0.558 ± 0.145
f_3	-0.598	-0.133	1.57	-0.731 ± 0.190
g_1	0.448	-0.031	1.55	0.417 ± 0.104
g_2	-0.493	0.096	1.61	-0.397 ± 0.099
g_3	-0.295	-0.329	1.63	-0.624 ± 0.150

Table 14: Parameters appearing in the fit function of the form factors and the values of the form factors at $q^2 = 0$ for $\Xi_c \to \Sigma \ell \nu$.

	a	b	m_{fit}	$q^2 = 0$
f_1	-1.498	2.075	1.60	0.577 ± 0.150
f_2	-0.359	-0.142	1.66	-0.501 ± 0.130
f_3	-0.760	0.082	1.70	-0.678 ± 0.176
g_1	0.159	0.292	1.57	0.451 ± 0.113
g_2	-0.317	-0.024	1.62	-0.341 ± 0.089
g_3	0.976	-1.218	1.62	-0.242 ± 0.061

Table 15: Parameters appearing in the fit function of the form factors and the values of the form factors at $q^2 = 0$ for $\Xi_c' \to \Xi \ell \nu$.

	a	b	m_{fit}	$q^2 = 0$
f_1	-0.564	0.640	1.52	0.076 ± 0.020
f_2	-0.226	-0.427	1.55	-0.653 ± 0.169
f_3	-1.007	0.112	1.58	-0.895 ± 0.232
g_1	-0.017	0.054	1.62	0.037 ± 0.009
g_2	-0.265	-0.081	1.60	-0.346 ± 0.089
g_3	0.238	-0.349	1.55	-0.111 ± 0.028

Table 16: Parameters appearing in the fit function of the form factors and the values of the form factors at $q^2 = 0$ for $\Xi_c' \to \Sigma \ell \nu$.

	$\Gamma(GeV)$
$\Xi_b \to \Xi e^+e^-$	$(9.941 \pm 2.982) \times 10^{-19}$
$\Xi_b \to \Xi \mu^+\mu^-$	$(9.872 \pm 3.455) \times 10^{-19}$
$\Xi_b \to \Xi \tau^+\tau^-$	$(1.611 \pm 0.483) \times 10^{-19}$
$\Xi_b \to \Sigma e^+e^-$	$(6.359 \pm 2.225) \times 10^{-20}$
$\Xi_b \to \Sigma \mu^+\mu^-$	$(6.194 \pm 2.167) \times 10^{-20}$
$\Xi_b \to \Sigma \tau^+\tau^-$	$(4.338 \pm 1.518) \times 10^{-20}$
$\Xi_c \to \Sigma e^+e^-$	$(2.162 \pm 0.757) \times 10^{-25}$
$\Xi_c \to \Sigma \mu^+\mu^-$	$(2.152 \pm 0.753) \times 10^{-25}$
$\Xi_c \to \Xi e^+\nu_e$	$(4.264 \pm 1.49) \times 10^{-13}$
$\Xi_c \to \Xi \mu^+\nu_\mu$	$(4.202 \pm 1.26) \times 10^{-13}$
$\Xi_c \to \Sigma e^+\nu_e$	$(2.204 \pm 0.771) \times 10^{-14}$
$\Xi_c \to \Sigma \mu^+\nu_\mu$	$(2.183 \pm 0.764) \times 10^{-14}$
$\Xi'_b \to \Xi e^+e^-$	$(2.411 \pm 0.843) \times 10^{-17}$
$\Xi'_b \to \Xi \mu^+\mu^-$	$(2.407 \pm 0.842) \times 10^{-17}$
$\Xi'_b \to \Xi \tau^+\tau^-$	$(1.199 \pm 0.419) \times 10^{-17}$
$\Xi'_c \to \Xi \mu^+\nu_\mu$	$(1.009 \pm 0.303) \times 10^{-12}$
$\Xi'_c \to \Xi e^+\nu_e$	$(1.109 \pm 0.388) \times 10^{-12}$
$\Xi'_c \to \Sigma e^+\nu_e$	$(8.425 \pm 2.948) \times 10^{-14}$
$\Xi'_c \to \Sigma \mu^+\nu_\mu$	$(8.340 \pm 2.919) \times 10^{-14}$
$\Xi'_c \to \Sigma e^+e^-$	$(1.718 \pm 0.515) \times 10^{-24}$
$\Xi'_c \to \Sigma \mu^+\mu^-$	$(1.666 \pm 0.499) \times 10^{-24}$
$\Xi'_b \to \Sigma e^+e^-$	$(3.815 \pm 1.335) \times 10^{-19}$
$\Xi'_b \to \Sigma \mu^+\mu^-$	$(3.813 \pm 1.334) \times 10^{-19}$
$\Xi'_b \to \Sigma \tau^+\tau^-$	$(2.783 \pm 0.974) \times 10^{-19}$

Table 17: The values of the decay rates in full theory for different leptons.

	BR
$\Xi_b \to \Xi e^+ e^-$	$(2.25 \pm 0.78) \times 10^{-6}$
$\Xi_b \to \Xi \mu^+ \mu^-$	$(2.23 \pm 0.67) \times 10^{-6}$
$\Xi_b \to \Xi \tau^+ \tau^-$	$(0.36 \pm 0.11) \times 10^{-6}$
$\Xi_b \to \Sigma e^+ e^-$	$(1.44 \pm 0.50) \times 10^{-7}$
$\Xi_b \to \Sigma \mu^+ \mu^-$	$(1.40 \pm 0.49) \times 10^{-7}$
$\Xi_b \to \Sigma \tau^+ \tau^-$	$(0.98 \pm 0.29) \times 10^{-7}$
$\Xi_c \to \Sigma e^+ e^-$	$(3.68 \pm 1.29) \times 10^{-14}$
$\Xi_c \to \Sigma \mu^+ \mu^-$	$(3.66 \pm 1.28) \times 10^{-14}$
$\Xi_c \to \Xi e^+ \nu_e$	$(7.26 \pm 2.54) \times 10^{-2}$
$\Xi_c \to \Xi \mu^+ \nu_\mu$	$(7.15 \pm 2.50) \times 10^{-2}$
$\Xi_c \to \Sigma e^+ \nu_e$	$(1.48 \pm 0.52) \times 10^{-2}$
$\Xi_c \to \Sigma \mu^+ \nu_\mu$	$(1.47 \pm 0.51) \times 10^{-2}$

Table 18: The values of the branching ratios in full theory for different leptons.